

Evaluation of the absorption capacity of the natural clay from Bikougou (Gabon) to remove Mn (II) from aqueous solution.

F. Eba^{1*}; S. Gueu²; A. Eya'A-Mvongbote¹; J. A. Ondo¹; B. K. Yao²; J. Ndong Nlo¹; R. Kouya Biboutou¹

1. Laboratoire Pluridisciplinaire des Sciences (LAPLUS) de l'Ecole Normale Supérieure de Libreville BP 17009 Libreville (Gabon).
2. Laboratoire de procédés industriels, de synthèse et de l'environnement, Département de Génie Chimique et Agroalimentaire, INP HB BP 1093 Yamoussoukro (Côte d'Ivoire).

Abstract :

The eventual use of the clay from Bikougou as an adsorbent for the removal of metal ions such as manganese, from aqueous solution, was investigated by the mean of batch technique. The results of adsorption were fitted to the Langmuir, Freundlich and DKR models. Satisfactory agreement between experimental data and the model predicted values was expressed by the correlation coefficient (R^2).

The Langmuir model represented the adsorption process better than Freundlich and DKR models, with correlation coefficients (R^2) values ranged from 0.97 to 0.99. The adsorption capacity (q_m) calculated from Langmuir was 10 mg/g for Mn (II) at pH 4 at 308K. The interaction adsorbate-adsorbent was found to be accompanied by positive values of enthalpy, entropy and negative values of Gibbs free energy.

The kinetics of Mn (II) ions adsorption followed the pseudo second-order model, because of its best correlation coefficients (ranged from 0.97 to 0.999) and higher agreement between q_e and q_{exp} .

Keywords: clay, adsorption capacity, isotherm pseudo-second-order.

I. Introduction

Heavy metals are thrown out from production processes of many industries. Metallurgical, hydrometallurgical, and pyrometallurgical technologies, give rise heavy metals in their effluents (Wojtowicz et al., (2002)). The presence of heavy metals in aquatic environment because of their toxic nature and other adverse effects on receiving ecosystems has been of great concern to scientific community (e.g., Bin Yu et al., 2000 and Ahmad et al., 2009). It follows that heavy metals need to be removed before the effluents stocked at adapted sites or reversed at rivers. The treatment of rich heavy metal aqueous solutions is realizable by mean of many methods including: ion exchange, chemical precipitation, ultrafiltration, electrochemical deposition, among which, adsorption on appropriate adsorbent (low cost and abundance of the latter) is one of the most efficient in terms of simplicity and feasibility of operation and low consumption of energy (Almeida et al., 2009). Adsorption process, known since the 17th century, characterises some porous materials to be capable to adsorb gas or chemical species into solutions (Fernandes et al., 2007).

During adsorption processes, pollutants are fixed at the surface of the adsorbents, separating them from liquid phase. Adsorption capacities of many adsorbents have been evaluated, such as sugar beet pulp and sawdust (e.g., Ajmal et al., 1998 and Chung et al., 1992), coconut shell (Sekar et al., 2004), red mud (Apek et al., 1998), husk (Gupta et al., 2006), deoiled soya (Gupta et al., 2008), activated carbon (Bouberka et al., 2006). Clay materials have already been shown to have high adsorption capacity, which may even exceed that of activated carbon under the same conditions of temperature and pH, because of their high specific surface area, high cation exchange capacity, Brönsted and Lewis acidities and positive or negative surface charge against pH (Lin et al., 2002). Many studies have been reported on the use of clays for metal ions removal from aqueous solutions: Zn(II) with natural bentonite (Mellah et al., 1997); Zn(II), Cd(II), Pb(II), with raw smectite (Wojtowicz et al., 2002), Pb(II) with carbonate rich illite (Li et al., 2001), Pb(II), Cd(II) and Ni(II) with montmorillonite and kaolinite (Gupta et al., 2008), Cd(II) and Zn(II) with montmorillonite (Beytia et al., 1996), Pb(II), Ni(II), Cr(VI) and Cu(II) with palygorskite (Potgieter et al., 2006), Cd(II) with palygorskite (Wang et al., 2007), Cu(II) with kaolinite (Alkan et al., 2008), lead(II) with bentonite (e.g.

Ayari et al., 2007 and Zhu et al., 2008), Cd(II) with bentonite (Panday et al., 1988), Pb(II) with palygorskite (Qiaohui Fan et al., 2009), Cu(II) and Cd(II) with bentonite (Karapinar et al., 2009), Ni(II) and Cu(II) with montmorillonite (Isagbemi et al., 2009) and various forms of modified clays also have been used (e.g. Zhu et al., 1998 and Krishna et al., 2000).

The purpose of the present study is to provide adsorption capacity of a natural mixture kaolinite, montmorillonite-illite sample of clay from Bikougou deposit (Gabon 11°37' E and 1°58' N) to remove Mn (II) from aqueous in a single batch system under various conditions.

II. Materials and methods.

II.1. Adsorbent.

X Rays and chemical analyses experiments performed at Nancy University (France) have been completed by those on determination of specific surface area (SSA), according to methylene blue method (Pham Thi Hang et al., 1970), cation exchange capacity by using ammonium acetate methods respectively (Rémy et al., 1976) acid and alkaline surface functional groups by means of Boehm titration (Rockstraw, 2000) and point of zero charge with the employment of potentiometric titration (Isagbemi et al., 2009).

II.2. Adsorbate and aqueous solution.

Mn (II) ($\text{MnCl}_2 \cdot 4\text{H}_2\text{O}$, MW 197, $90\text{g}\cdot\text{mol}^{-1}$) was used as the adsorbate in this study. Obtained from Prolabo (Analytical grade), it was used without further purification. Aqueous solutions of Mn (II) were prepared by dissolving an accurately weighed amount of $\text{MnCl}_2 \cdot 4\text{H}_2\text{O}$ in distilled water to achieve concentrations of Mn (II) (ranged from 19mg/L to 120mg/L).

II.3. Adsorption procedure.

The adsorption of Mn (II) ions on to clay from Bikougou was studied by the mean of batch technique.

The procedure used for this study is described as following: a known weight (0.25 mg) of clay was equilibrated with 50 mL of the spiked manganese solution of known concentration, in a stopped propylene flask, at a fixed temperature and in a thermostatic shaker for a known period time. After the equilibration using a constant stirring speed, the suspension was filtered out and analysed for its manganese concentration, using atomic adsorption spectrometer (Analyst 100 Perkin Elmer).

The effect of several parameters such as pH, contact-time, initial concentration of manganese solutions and temperature on the adsorption was studied following different sets of experiments:

Effect of pH:

Clay: 5 g/L; Mn (II): 31.25 mg/L; temperature: 301K; interaction-time: 45 min; pH: 2-8 and 2 units intervals.

Effect of initial Mn (II) concentration and adsorption isotherm:

Clay: 5 g/L; temperature: 308K, 313K and 318K; contact-time: 45 min; pH: 4; Mn (II) solution: 19, 23, 31, 38, 67, 83, 98, 117 mg/L.

Kinetic studies:

Clay: 5 g/L; temperature: 308K, 313K and 318K; Mn (II): 67 and 83 mg/L; pH: 4; interaction-time: 5, 10, 15, 25, 35, 45 min

II.4. Calculs.

The percent adsorption (% ads) and the amount of Mn (II) ions adsorbed per unit mass of adsorbent (q_t) were calculated by using respectively the following equations:

$$(\% \text{ ads}) = \frac{C_0 - C_t}{C_0} \times 100 \quad (i)$$

and

$$q_t = (C_0 - C_t) \times \frac{V}{m} \quad (\text{ii})$$

where C_0 and C_t are the initial Mn(II) concentration and Mn(II) concentration at any time contact of interaction adsorbate-adsorbent; V is the volume of manganese solutions and m is the mass of clay.

III. Results and discussion.

III.1. Characterization of adsorbent

The results concerning chemical analyses, modal composition, cation exchange capacity (CEC), specific surface area (SSA), pH of point zero charge (PZC), acid and alkaline surface functional groups, are reported in tables 1, 2 and 3 respectively; The XRD patterns of crude clay and clay fractions enabled us to determine the qualitative mineralogical composition of the material. From X-ray diffraction patterns (figures 1 and 2), it appears that it comprises the following minerals:

- Kaolinite; its ray at 7.19 Å in untreated clay is shifted at 10.40 Å by hydrazine saturation (figure 2, curve H). The latter disappears on heating at 490°C (figure 2, curve C). In figure 1, other rays of kaolinite are at 3.59 Å, 2.56 Å and 2.73 Å;
- Dioctahedral smectite: typical rays are at 14.93 and 4.45 Å (figure 1) or at 15.13 Å (Figure 2, curve U); based on its d_{001} at 14.93 Å or at 15.13 Å, we suggest that calcium is the main interlayer cation (Deer et al., 1992). The treatment with ethylene-glycol shifted the d_{001} at 17 Å (Figure 2, curve G) whereas on heating this d_{001} is reduced to 9.80 Å (figure 2, curve C);
- Feldspars are revealed by reflections at 3.18, 3.21, 4.04 Å. The pattern is typical of andesine or albite.
- Illite-like materials displaying a d_{001} at 9.97 Å (figure 1) or at 10.02 Å (figure 2, curve U), which is not affected by the above-mentioned treatments (figure 2). Other illite rays are at 5.01 Å, 4.45 Å, 3.88 Å, 3.65 Å, 3.34 Å, 2.87 Å, 2.56 Å in figure 1.
- Quartz; 3.34 Å, 4.27 Å, 2.81 Å ;
- Calcite (3.05 Å, 3.86 Å). When the material is acid treated (HCl, 5 %), these rays disappear (figure 2) ;
- anatase; (3.51 Å, 2.37 Å, 1.89 Å);
- maghemite; (2.93 Å, 2.56 Å);
- Ba, Sr-hydroxyapatite (4.45 Å, 3.76 Å, 1.82 Å, 2.13 Å, 2.93 Å).

By combining the X-ray results and the whole-rock chemical analyses, the modal compositions of untreated clay can be estimated according to a constrained multi-linear calculation as reported by Njopwouo, (1984) and Yvon et al., (1990) using the following basic formula:

$$T(a) = \sum_1^n M_i \times P_i(a) \quad \text{where}$$

$T(a)$ = wt.% element "a" in the sample;

M_i = wt.% mineral "i" in the sample, and

$P_i(a)$ = proportion of element "a" in the mineral "i".

III.2. Effect of pH.

The effect of pH on the adsorption of Mn (II) ions on to clay from Bikougou was studied by varying it in the range of 2-8 as shown in table 4. The uptake of Mn (II) ions depends of pH, it increases with the increase of pH, from 2 to 8: (i) substantially from 2 to 4, (ii) very slowly from 4 to 6 and (iii) substantially again from 6 to 8.

These results demonstrated the importance of pH on the mechanism governing the adsorption characteristics of heavy metals on clays, known as given by dissolution (weak pH), ion exchange adsorption and precipitation (high pH) (Ho et al., 2002). Many studies revealed that the removal efficiency of heavy metals by clays decreases at lower pH values ($\text{pH} < 4$) and increases at pH values up of 4 (e.g., Hasany et al., 1998 ; Juang et al., 1997 and Erdem et al., 2004).

This behaviour is confirmed at this study.

The basis mechanism that governs the adsorption characteristics of clay from Bikougou

(i) at lower pH than pH of point zero charge ($\text{PZC} = 3.2 \pm 0.2$) is adsorption and (ii) at higher pH than pH of point zero charge is adsorption and ion exchange. So at these pH levels (4-8), the alkaline, alkaline earth and acid cations

located in the exchangeable sites of clay (Na^+ , K^+ , Ca^{2+} , Mg^{2+} , Al^{3+} , Fe^{3+} , H^+) are replaced by Mn (II) ions present in prepared aqueous solution. It appears that, as pH changes, the surface functional also changes and the sorption of charged species is affected. It is convenient that at lower pH values ($\text{pH} < \text{PZC}$), where there is an excess of H_3O^+ ions, in the solution, a competition exists between the positively charged hydrogen ion and Mn (II) ions for the available sites on the negatively charged clay surface, according to Mathialagan et al., (2002).



This positive surface charge interacts repulsively with approaching Mn (II) cations and prevents them from reaching the surface and thus, the adsorption was not much at low pH.

At higher pH ($\text{pH} > \text{PZC}$), the clay surface becomes negatively charged because of deprotonation of functional group favouring Mn^{2+} uptake



As the pH increases (4- 7) and balance between H_3O^+ and OH^- gives OH^- excess, more of Mn (II) ions in the solution are adsorbed on the negative clay surface and thus the removal percentage of Mn (II) ions adsorbed increases. When the pH becomes alkaline ($\text{pH} > 7$) possible precipitation of insoluble trioxide Mn_2O_3 may occur as higher metal removed.

From this consideration, the experiments on the adsorption of Mn (II) ions on clay were realized at a pH of 4.

III.3. Effect of initial manganese concentration.

The effect of initial Mn (II) ions concentration on the adsorption onto clay from Bikougou is reported in table 5. Hence, it is observed that more Mn (II) ions were progressively retained by the clay, and the adsorption process became efficient, as the initial Mn (II) ions concentration increased, up to obtain constant amounts adsorbed at higher initial concentration. Similar results have also been reported by Gupta et al.,2008.It appears that ,at low Mn(II) ions concentration ,number of available adsorption sites is very high comparatively to that of Mn(II) ions ,amounts of Mn(II) ions adsorbed is weak .When the concentration of Mn(II) ions increases, because of presence of an elevated number of Mn (II) ions in solution ,the amount of Mn(II)ions increases. The adsorption equilibrium is established when the amount of Mn(II) ions fixed at the interface solid solution is in dynamic balance with that on surface.

III.4. Effect of reaction time

From fig 3. , it can be seen that the adsorption of Mn (II) ions adsorbed increased with in creasing time of equilibration. The removal of Mn (II) increased with time to obtain equilibrium at about 30 min. After that, contact time has not effect in metal removal percentage. Very high adsorption rates were observed at the beginning because of the great number of sites available for the sorption operation and adsorption equilibrium were then gradually achieved as reported by Bedoui et al., 2008.

III.5. Adsorption isotherms studies.

The experimental adsorption data have been subjected to different adsorption isotherms namely Langmuir (I. Langmuir, 1918), Freundlich (Ho et al., 2002) and Dubinin-Kaganer-Radushkevich (DKR) (Hasany et al., 1998) models in the aims (I) to determine the adsorption capacity of clay from Bikougou as adsorbent and (II) to obtain both a good picture of the surface and best interpretation of adsorption process.

The Langmuir isotherm, expressed in its linearized form by the equation:

$$\frac{C_e}{q_e} = \frac{1}{bq_m} + \frac{C_e}{q_m} \quad (III)$$

is applicable if the monolayer coverage of adsorbent with adsorbate takes place on a homogeneous adsorbent surface. The Langmuir coefficients b and q_m representing respectively the adsorption equilibrium constant and maximum adsorption capacity have been determined from the intercepts and slopes of the plots $\frac{C_e}{q_e}$ vs C_e (Fig. 4), which are linear.

The absorption equilibrium constant b values varied from 17.5 to 80 L/g and maximum adsorption capacity values were ranged from 10 to 11.36 with the increase in temperature from 308K to 318K. The correlation coefficients (R^2) were remained between 0.99 and 0.97.

The study of Langmuir isotherm has been completed by that of dimensionless constant R_L , called equilibrium constant (Juang et al., 1997).

$$R_L = \frac{1}{1 + bC_0} \quad (IV)$$

The R_L values indicate the type of isotherm: to be favourable $0 < R_L < 1$, linear ($R_L = 1$) or irreversible ($R_L = 0$). The R_L values issued from this study were ranged between 0.3125 and 0.328 at 308K and between 0.158 and 0.223 at 318K. These results have indicated that the description of adsorption process by mean of Langmuir model is favourable.

The linearized form of the Freundlich isotherm is given by the equation:

$$\ln q_e = \ln K_F + \frac{1}{n} \ln C_e \quad (V)$$

This equation predicts multilayer adsorption on heterogeneous surface, characterized by an exponential distribution of active sites. The Freundlich coefficients k_F and n corresponding respectively to adsorption capacity and adsorption intensity have been obtained from the intercepts and slopes of linear plots $\ln q_e$ against $\ln C_e$ (Fig. 5). The adsorption capacity (k_F) and adsorption intensity (n), were found varying respectively from 0.4786 mg/g at 308K, to 7.36 mg/g at 318K and from 1.46 to 5.2 in relation with the increasing temperature from 308K to 318K and with correlation coefficients (R^2) ranged between 0.98 and 0.935. The values of the adsorption intensity obtained in conformity with the requirement $n > 1$ for physical adsorption process (Ijagbemi et al., 2009), characterized the nature favourable of the adsorption of Mn (II) ions onto clay of Bikougou described by the Freundlich isotherm.

The DKR equation has been widely used to explain energetic heterogeneity of solid at low coverages as monolayer regions in micropores (e.g., Karapinar et al., 2009 and Krishna et al., 2000). The equation of the DKR model is given by the expression:

$$\ln q_e = \ln X_m - \beta \varepsilon^2 \quad (VI)$$

where β is the activity coefficient related to mean adsorption energy, X_m the maximum of adsorption capacity and ε is the Polangi potential, which is equal to

$$\varepsilon = RT \ln(1/C_e) \quad (VII)$$

with:

R: as the gas constant (kJ/mol/K)

T: as the temperature (K)

The saturation limit X_m may represent the total micropore volume of the adsorbent.

The adsorption potential is independent of temperature but varies according to the nature of adsorbent and adsorbate.

The adsorption energy E expressed by the equation:

$$E = -\frac{1}{(-2\beta)^{0.5}} \quad (VIII)$$

Reveals the nature of adsorption. If the value of adsorption energy E is ranged between -1 and -8 kJ/mol, adsorption process is physical, and if the value of E is ranged between -9 and -16 kJ/mol, it is chemical adsorption.

The DKR parameters E and X_m were calculated from the slopes and intercepts of the linear plots linear of $\ln q_e$ versus ε^2 (Fig.6).

The adsorption energy E values obtained:- 6.22 kJ/mol at 308K,- 6.35 kJ/mol at 313K and -11.11kJ/mol at 318K, were in the same range of those obtained from the adsorption of Mn^{2+} (- 8.8 kJ/mol at 303K) on natural zeolites (Erdem et al., 2004) when physioadsorption (-1 - 8 kJ/mol) controlled the process (Saeed, 2003). Chemical process

(E ranged between - 9 and -16 kJ/mol) appeared since 318K. The adsorption capacity in DKR equation was found to be varying from 1.8 mg/g at 308K to 9.87 mg/g at 318K with correlation coefficients up 0.9 (0.91 at 318K, 0.96 at 313K and 0.99 at 308K).

The comparative testing of isotherm models performed by the consideration both of the best correlation coefficients and the satisfactory agreement between maximum adsorption capacity (q_m in Langmuir model, K_F in Freundlich model and X_m in DKR model) with experimental data, had demonstrated that if these three models could well describe the adsorption process, best results have been obtained with the Langmuir model (Table 6) at any explored temperature (308K, 313K and 318K). This illustrates that the adsorption occurs through the formation of a monolayer coverage of Mn(II) ions on the surface of the clay. Nevertheless, the amelioration of adsorption capacity for DKR model ($X_m = 1.83$ mg/g at 308K, 3.06 mg/g at 313K and 9.87 mg/g at 318K) and Freundlich isotherm ($k_F = 0.47$ mg/g and $n = 1.48$ at 308K, $K_F = 0.79$ mg/g and $n = 1.49$ at 313K; $K_F' = 7.36$ mg/g and $n = 5.26$ at 318K) up 313K, suggested the adsorbent surface became progressively heterogeneous as a result of appearance of chemical adsorption process (Saeed, 2003).

III .6. Thermodynamics parameters.

The adsorption of Mn (II) ions on the clay from Bikougou, increased as function of temperature from 308K to 318K. Similar result was also found for the adsorption of copper by kaolinite (Alkan et al., 2008). The process is controlled by the adsorbate-adsorbent interaction.

The Langmuir constant b, was used to estimate the enthalpy, entropy and Gibbs energy charges accompanying adsorption, from the following relationships:

$$\Delta_{ad}G^{\circ} = -RT\ln b \quad (IX)$$

$$\text{and } \ln b = -\frac{\Delta_{ad}H^{\circ}}{RT} + \frac{\Delta_{ad}S^{\circ}}{R} \quad (X)$$

Where $\Delta_{ad}H^{\circ}$ and $\Delta_{ad}S^{\circ}$ are respectively the variation of enthalpy and that of entropy issued of adsorption process. The plot of $\ln b$ as a function of T (K)⁻¹ is shown in figure 7. From the slope and intercept of the corresponding linear curve obtained, the enthalpy ($\Delta_{ad}H^{\circ}$) and entropy ($\Delta_{ad}S^{\circ}$) values were determined. Gibbs free energy ($\Delta_{ad}G^{\circ}$) was calculated by using the widely known equation.

$\Delta_{ad}G^{\circ} = \Delta_{ad}H^{\circ} - T\Delta_{ad}S^{\circ}$ If that is the case, the values of thermodynamics parameters were:

(i) $\Delta_{ad}H^{\circ} = 0.1157$ kJ/mol,

(ii) $\Delta_{ad}S^{\circ} = 342.56$ J/K/mol.

(iii) $\Delta_{ad}G^{\circ}$ decreased from -105.39 kJ/mol at 308K to -107.10 kJ/mol at 313K and -108.82 kJ/mol at 318K. This result illustrates that the adsorption phenomenon is more efficient with the increase in temperature.

The positive value of $\Delta_{ad}H^{\circ}$, indicates the endothermic nature of the adsorption process. The positive change of entropy corresponds to the fixation of Mn (II) ions at the exchange sites of the randomly distributed surfactant species and also that the adsorption is irreversible (Ho et al., 1999b). The negative value of Gibbs free energy indicated that the process is spontaneous.

IV. Kinetic studies.

IV.1. Adsorption order.

The model of pseudo first order and that of pseudo second order were tested for the determination of adsorption process order. These models are given respectively by the equation:

$$\log(q_e - q_t) = \log q_e - \frac{k_1}{2.303} t \quad (XII)$$

$$\text{and} \quad \frac{t}{q_t} = \frac{1}{k_2 q_e^2} + \frac{t}{q_e} \quad (\text{XIII})$$

where: (I) k_1 and k_2 are respectively the rate constant of pseudo first order adsorption (mn^{-1}) and that of pseudo second order adsorption ($\text{g/mg}^2 \cdot \text{mn}$),

(II) q_e and q_t the amounts of Mn(II) ions adsorbent at equilibrium (mg/g) and at various times respectively.

The kinetic parameters, obtained from the slopes and intercepts of linear plots $\log(q_e - q_t)$ versus t (Fig.8) and t/q_t as a function of t (Fig.9) were reported in table 7.

The validity of kinetic model is supported by the employment of two parameters: (i) correlation coefficients values and (ii) good agreement between experimental data (q_{exp}) and model predicted values of the amounts of Mn (II) ions adsorbed (q_e). Satisfactory model has good linearity of plots ($R^2 > 0.9$) and highest agreement between q_e and q_{exp} (small deviation).

The results showed (i) the high correlation coefficients ($R^2 > 0.9$ in all cases) for the pseudo second order comparatively of those of pseudo first order (R^2 varying from 0.13 to 0.87 when temperature increases from 308K to 318K); (ii) A progressive better concordance between q_e and q_{exp} for the pseudo second order model at 313K and 318K (deviation varying from +0.05% to -0.11% at 313K, from 0.03% to -0.027% at 318K) while that of the pseudo first order model is very weak (deviation varying from -68.43% to -89.38% at 313K, and from -47.05 to -77.98% at 318K).

These results indicated that the adsorption kinetic of Mn (II) ions on to clay of Bikougou followed the pseudo second order kinetic model.

IV.2. Kinetic mechanism.

The mechanism of kinetic adsorption had been studied by applying experimental data to:

(i) pseudo second order model, (ii) liquid film diffusion model (Boyd et al., 1947) and (iii) intra-particle diffusion model (Keith et al., 2004)

Their corresponding equations are given by the expressions respectively:

$$\text{for the intra-particle diffusion: } q_t = k_3 t^{0.5} \quad (\text{XIV})$$

$$\text{and: for the liquid diffusion: } -\ln\left(1 - \frac{q_t}{q_e}\right) = k_4 t \quad (\text{XV})$$

Where k_3 and k_4 are respectively the intra-particle diffusion and liquid film diffusion rate constants.

The parameters of each model have been calculated from the slopes and intercepts of linear plots q_t vs $t^{0.5}$ and $-\ln(1 - q_t/q_e)$ vs t respectively (Fig. 10 and 11 respectively). The results are reported in table 8.

If the intra-particle diffusion or the liquid film diffusion was the adsorption mechanism model, the plots might have zero intercept (varies from 1.96 to 1.56 for intra-particle diffusion model and from 0.4 to 0.236 with liquid film diffusion model) and passed through the origin (Gupta et al. 2008). Despite, the plots being linear, the correlation coefficients (R^2) of intra-particle diffusion model (0.66 to 0.9) < of pseudo second order (0.999 to 0.97) and of liquid film diffusion (0.72 to 0.83) < of pseudo second order (0.999 to 0.97), show that the experimental data did not fit the equation of intra-particle diffusion model q_t vs $t^{0.5}$ or that of liquid film diffusion model $-\ln(1 - q_t/q_e)$ vs t . Large intercepts obtained by using intra-particle diffusion model suggested that the process was largely surface adsorption and not intra-particle diffusion phenomena. The small intercepts of plots $-\ln(1 - q_t/q_e)$ vs t , could be considered as a suggestion that liquid film diffusion model might have some role to play in the kinetics of adsorption of Mn(II) ions onto clay from Bikougou.

The test of different models of adsorption mechanism had presented that mechanism issued of pseudo second order model had given the best fit of experimental data and consequently, the adsorption of Mn (II) ion on to crude clay of Bikougou could be considered following a mechanism related to the pseudo second order kinetic model.

V. Conclusion.

This study proved that Mn (II) could be adsorbed and thus removed in significant amount by crude clay of Bikougou from aqueous solutions.

In batch method, removal of Mn (II) ions increased with the increase of contact time (45 mn of contact-time are sufficient), amount of Mn (II) in solution, pH and temperature.

The equilibrium data could be described by the Langmuir, Freundlich and DKR equations. However, the Langmuir model better represented the adsorption process than Freundlich and DKR models.

At a pH of 4 and temperature T (K) $\geq 308K$, adsorption occurred was found not to be a spontaneous physioadsorption process.

Kinetic modelling results showed that the pseudo second order equation was appropriate for the description of this type of adsorption and removal both concerning the determination of order and mechanism of reaction.

VI. References.

- [1] Ahmad, A.; Rafatullah, M.; Suliman, O.; Hakimi Ibrahim, M.; Yap Yee, C.; Siddique Bazlul, M., (2009). Removal of Cu (II) and Pb (II) ions from aqueous solutions by adsorptions on sawdust of Merantiwood: *Desalination*, 247, 636-646.
- [2] Ajmal, M.; Khan, A.H.; Ahmad, S.; Ahmad A., (1998). Role of sawdust in the removal of copper (II) from industrial wastes: *Water Research*, 32 3085-3091.
- [3] Alkan, M.; Kalay, B.; Dogan, M.; Demirbas, O., (2008). Removal of copper ion from aqueous solutions by kaolinite and butch design: *Journal of Hazardous Materials*, Vol. 153, N°1-2, 867-876.
- [4] Almeida, C.A.P.; Debacher, N.A.; Downs, A.J.; Cottet, L.; Mello, C.A.D., (2009). Removal of methylene blue from colored effluents by adsorption on montmorillonite clay: *Journal of colloid and interface science* 332, 46-53.
- [5] Apek, R.; Tuten, E.; Hugul, M.; Hizal M., (1998). Heavy metal cations retention by unconventional sorbents (red muds and fly ashes): *Water Research*, 32, 430-440.
- [6] Ayari, F.; Srasra, E.; Trabelsi-Ayadi, M., (2007). Retention of lead from aqueous solution by use of bentonite as adsorbent for reducing leaching from industrial effluents: *Desalination*, Vol. 206, N°1-3, 270-278.
- [7] Bedoui, K.; Bekri-Abbes, I.; Srasra, E., (2008). Removal of Cadmium (II) from aqueous solution using pure smectite and Lewatite S 100: the effect of time and metal concentration: *Desalination*, 223, 269-273.
- [8] Bin Yu, Zhang, Y.; Shukla Alka; Shyam Sukla, S.; Dorris Kenneth, L., (2000). The removal of heavy metal from aqueous solutions by sawdust adsorption-removal copper: *Journal of Hazardous Materials B80* 33-42.
- [9] Bouberka, Z.; Khenifi, A.; Benderdouche, N.; Derriche, Z., (2006). *J. Hazard. Mater.* 133 154.
- [10] Boyd, G.E.; Adamson, A.W.; Mye, R.S.Jr, (1947). The exchange adsorptions of ions from aqueous solutions on organic zeolites: *Journal of American Society*, G9 2836-2842.
- [11] Chung, Y.S.; Lee, K.W.; Yoon, Y.S.; Kwon, S.H.; Lim, K.S., (1992). The adsorption behaviour of heavy metal ions on sawdust: *Bulletin of the Korean Chemical Society*, 13 212-214.
- [12] Deer, W. A.; Howie, R. A.; Zussman, J., (1992). *An introduction to the rock-forming minerals: Second edition*, London, 696 p.
- [13] Erdem, E.; Karapinar, N.; Donat, R., (2004). The removal of heavy metal cations by natural zeolites: *Journal of Colloid Science*, 280, 309-314.
- [14] Fernandes, A.N.; Almeida, C.A.P.; Menezes, C.T.B.; Debacher, N.A.; Sierra, M.M.I., (2007). *J. Hazard. Mater.* 144, 412.
- [15] Gupta Susmita, S.; Bhattacharyya, K., (2008). Immobilization of Pb (II), Cd (II) and Ni (II) ions on kaolinite and montmorillonite surface from aqueous medium: *Journal of Environmental Management*, 87, 46-58.
- [16] Gupta, V.K.; Mittal, A.; Gajbe, V.; Mittal, J., (2008). *Journal of Colloid Interface Science*, 319 103.
- [17] Gupta, V.K.; Mittal, A.; Jain, R.; Mathur, M.; Sikarwar, S., (2006). *Journal of Colloid Interface Science*, 303, 80.
- [18] Hasany, S.M.; Chaudhry, M.H., (1998). Fixation of Cr (III) traces onto Haro rivers and from acid solutions: *J. Radioanal. Nucl.Chem.*, 230 N°11.
- [19] Ho, Y.S.; Huang, C.T., (2002). Equilibrium sorption isotherm for metals ions on tree fern: *Process Biochemistry*, 37, 1421-1430.
- [20] Ho, Y.S.; Mc Kay, G., (1999)a. Pseudo second order model for sorption processes: *Process Biochemistry*, 34, 451-465.
- [21] Ho, Y.S.; Mc Kay, G., (1999)b. Batch lead (II) removal from aqueous solution by peat: equilibrium and kinetics. *Transactions of the Institution of Chemical Engineers* 76B, 332- 339.
- [22] Juang, R.S.; Wu, F.C.; Tseng, R.L., (1997). Ability of activated clay for the adsorption of dyes from aqueous solutions: *Environ. Technol.*, 18, 535.
- [23] Karapinar, N.; Donat, R., (2009). Adsorption behaviour of Cu^{2+} and Cd^{2+} onto natural bentonite: *Desalination*, Vol. 249, N°1, 123-129
- [24] Keith, K.H.; Choy; Porter, J.F.; Mc Kay G., (2004). Film-pore diffusion models analytical and numerical solutions: *Chemical Engineering Science*, 59, 501-512.
- [25] Krishna, B.S.; Murty, D.S.R.; Prakash, B.S.J., (2009). Thermodynamics of chromium (VI) anionic species sorption onto surfactant-modified montmorillonite clay: *J. Colloid Interf. Sci.*, 229 230.
- [26] Langmuir I., (1918). The adsorption of gases on plane surfaces of glass, mica and platinum: *J. Am. Chem. Soc.* Vol.40 ,(9), 1361-1403.
- [27] Lin Su-Hsia; Juans Reuy-Shin, (2002). Heavy metal removal from water by sorption using surfactant-modified montmorillonite: *J. Hazard. Mater.* B92, 315-326.
- [28] Li, R.S.; Yong, R.N.; Li, L.Y., (2001). Mathematical prediction of lead removal from carbonate-rich illite: *Geoenvironmental Engineering* Vol. 60, N°1-4, 159-171.
- [29] Mathialagan, T.; Viraraghavan, T., (2002). Adsorption of cadmium from aqueous solution by perlite: *Journal of Hazardous materials*, 94, 291- 303.
- [30] Mellah, A.; Chegrouche, S., (1997). The removal of zinc from aqueous solutions by natural Bentonite: *Water Research* ,Vol. 31, N°3, 621-629.
- [31] Njopwouo, D., (1984). *Minéralogie et physico-chimie des argiles de Bomkoul et de Balengou (Cameroun). Utilisation dans la polymérisation du styrène et dans le renforcement du caoutchouc naturel*, Thèse Doct. Etat. Fac. Sci., Université de Yaoundé, 300 p.
- [32] Olakitan, I.C.; Mi-Hwa Baek ; Dong-Su, K., (2009). Montmorillonite surface properties and sorption characteristics for heavy metal removal from aqueous solutions: *Journal of Hazardous materials*, Vol. 166, n°4, 538-546.
- [33] Panday, K.K.; Prasad, G.; Singh, V.N., (1998). *Environ. Technol.* Lett. 9, 1153-1162.
- [34] Pham, T.H. ; Windley, G.W., (1970). Methylene blue absorption by clay minerals. Determination of surface area and cation exchange capacities: *Clays and clays minerals*, Vol. 18, 203-212.

- [35] Potgieter, J. H.; Potgieter-Vermaak, S.S.; Kalibantonga, P.D., (2004). Heavy metal removal from solution by palygorskite clay: Minerals Engineering, Vol. 19, N°5, 463-470.
- [36] Quiohui Fan; Zhan Li; Haoguizhao; Zehog Jia; Jungzheng Xu; Wangsuo Wu, (2009). Applied Clay Science, Vol. 45, N°3, 111-116.
- [37] Rémi, J.C. ; Orsini, L., (1976). Utilisation du chlorure de cobalthexamine pour la détermination simultanée de la capacité d'échange et des bases échangeables dans les sols: Sciences de sol, 4, 269-275.
- [38] Rockstraw, D.A.; (2000). Characterization of Pecan shell-based carbon: Technical completion Report, November 2000, New Mexico State University, Las Cruces, Chemical Engineering.
- [39] Saeed, M.M., (2003). J. Radioanal. Nucl. Chem., 256, 73-76.
- [40] Sekar, M.; Sakthi, V. ; Rengaraj, S., (2004). Kinetics and equilibrium adsorption study of lead (II) onto activated carbon prepared from coconut shell: Journal of Colloid Interface Science, 279, 307-313
- [41] Shujing, Z.; Haobo, H.; Yongjie, X., (2008). Kinetic and isothermal studies of lead ion adsorption onto bentonite: Applied Clay science, Vol. 40, N°1-4, 171-178.
- [42] Undabeytia, T.; Morrillo, E.; Maqueda, C., (1996). Clays Clay Miner, 31, 485-490.
- [43] Wang, W.; Chen, H.; Wang, A., (2007). Adsorption characteristics of Cd (II) from aqueous solution onto activated palygorskite: Separation and Purification Technology, Vol.55, N°2, 157-164.
- [44] Wójtowicz, A.; Stoklosa, A., (2002). Removal of heavy metals on Smectite ion-exchange column: Polish Journal of Environmental Studies, Vol 11. N°1, 97-101.
- [45] Yvon, J.; Baudracco, J.; Cases, J.M.; Weiss, J., (1990). Eléments de minéralogie quantitative en micro-analyse des argiles. In: Matériaux Argileux, Structures, Propriétés et Applications. SFMC – GFA, Paris. Decarreau A. éditeur, ISBN 2-903589-06-02, Partie IV, Chap. 3, 473-489.
- [46] Zhu, L.; Ren, X.; Yu, S., (1998). Use of cetyltrimethylammonium bromide-bentonite to remove organic contaminants of varying polar character from water: Environ. Sci. Technol. 32, 3374.

Table 1 Chemical composition of clay material from Bikougou

SiO ₂ wt%	54.32	As ppm	< L.D.	Eu	115	Ni	29.26	U	0.40
Al ₂ O ₃	24.64	Ba	357.80	Ga	27.45	Pb	7.06	V	97.89
Fe ₂ O ₃	3.87	Be	1.06	Gd	2.62	Pr	4.13	W	37.17
MnO	0.02	Bi	< L.D.	Ge	1.06	Rb	15.93	Y	9.02
MgO	0.60	Cd	< L.D.	Hf	2.21	Sb	< L.D.	Yb	0.75
CaO	2.53	Ce	36.67	Ho	0.32	Sm	3.29	Zn	56.69
Na ₂ O	3.09	Co	17.51	In	< L.D.	Sn	1.14	Zr	82.77
K ₂ O	0.89	Cr	61.45	La	19.86	Sr	505.60		
TiO ₂	0.90	Cs	0.51	Lu	0.11	Ta	0.40		
P ₂ O ₅	0.05	Cu	38.43	Mo	< L.D.	Tb	0.35		
LOI	8.35	Dy	1.87	Nb	6.42	Th	1.81		
Total	99.26	Er	0.83	Nd	17.25	Tm	0.12		

Table 2 Modal compositions of untreated clay material and clay fraction (wt %), see text. The composition of untreated clay is determined by combining qualitative X-ray data and chemical analysis while the composition of clay fraction is determined from X-ray pattern (Intensities measurements without absorption correction).

Mineral	Untreated clay	Clay fraction
Kaolinite	29.1	53.0
Albite	20.3	0
Montmorillonite	15.2	40.0
Illite	10.9	7.0
Quartz	19.1	0
Carbonates	3.0	0
Maghemite	1.2	0
Anatase	0.9	0
Ba-Sr hydroxyapatite	0.8	0
Zircon	trace	0

Table 3 Characteristics of Bikougou clay deposit

pH of point zero charge (PZC)	CEC (meq/100g)	Acidity neutralizations (meq/L)			Surface area (m ² /g)
		NaOH	NaHCO ₃	Na ₂ CO ₃	
3	12.87	2.79	0.285	0.0	170

Table 4 Amounts and percentages of Mn(II) adsorbed as function of pH (clay 5g/L; concentration Mn(II) solution 31.25 mg/L, time 45 mn).

pH 2		pH 4		pH 6		pH 8	
q _e (mg/g)	% ads						
1.22	19.52	5	80	5.10	81.6	5.534	88.54

Table 5 Amounts and percentages of Mn(II) adsorbed as function of initial concentration (clay 5g/L ; contact time 45 mn, pH4).

Initial concentration Mn(II) ions solution (mg/L)	19.76	23.387	31.25	37.5	66.67	83.33	98.15	116.6
q _e (mg/g)	3.5	4	5	5.8	9.87	11.11	10.05	10.72
% ads	88.56	85.57	80	77.33	74.02	66.66	53.49	46.14

Table 6 Langmuir, Freundlich and DKR parameters and statistical for adsorption of Mn(II) ions at 308K, 313K and 318K (initial concentration of Mn(II) ions solution 67, 83, 98, 117 mg/L, pH4, time 45 mn).

T(K)	Langmuir Isotherm					Freundlich Isotherm			DKR Model		
	q _{exp} (mg/g)	q _m (mg/g)	b (L/mg)	R _L	R ²	K _F (mg/g)	n	R ²	X _m (mg/g)	E (kJ/mol)	R ²
308	8.64 to 11.11	10	0.0175	0.3125 to 0.328	0.99	0.4786	1.48	0.98	1.813	-6.22	0.98
313	9.88 to 12.03	10.87	0.0395	0.23 to 0.286	0.99	0.794	1.49	0.99	3.06	-6.35	0.96
318	13.58 to 16.36	11.36	0.0811	0.158 to 0.223	0.97	7.36	5.263	0.935	8.87	-11.11	0.91

Table 7 Pseudo first order, pseudo second order constants (rate constant, amount of Mn adsorbed) and statistical for adsorption of Mn(II) ions (clay 5g/L, pH4) determination of reaction order.

T(K)	Initial concentration (mg/L)	Pseudo first order					Pseudo second order				
		q _{exp} (mg/g)	q _c (mg/g)	% deviation	k _{1*100} (mn ⁻¹)	R ²	q _c (mg/g)	% deviation	k _{2*100} (g/mg.min)	R ²	
308	66.66	9.87	6.606	-33.06	4.67	0.84	8.53	-18.8	0.8	0.99	
	83.33	11.11	8.313	-25	4.35	0.75	9.5	-14.49	0.59	0.97	
313	66.66	12.037	3.8	-68.43	6.909	0.87	12.65	+0.05	1.8	0.99	
	83.33	12.5	1.39	-89.38	5.76	0.13	11.11	-0.11	1.04	0.99	
318	66.66	13.58	7.19	-47.05	9.39	0.58	13.98	+0.03	6.02	0.97	
	83.33	15.12	3.33	-77.98	7.16	0.23	14.71	-0.027	3.64	0.99	

Table 8 Intraparticle diffusion and liquid film diffusion rate constants coefficients (clay 5g/L, pH4).

Models	Parameters and statistical	Initial concentration of Mn (II) ions solutions (mg/L)			
		66.66		83.33	
		308K	313K	308K	313K
Intraparticle diffusion	k_3 (mg/g.min ^{0.5})	1.24	0.23	1.3	0.24
	Intercepts	1.96	9.2	1.66	9.67
	R ²	0.9	0.07	0.86	0.23
Liquid film diffusion	k_4 (mn ⁻¹) *100	4.62	13.8	4.69	1.12
	Intercepts	0.401	0.0524	0.23	1.87
	R ²	0.83	0.85	0.76	0.25

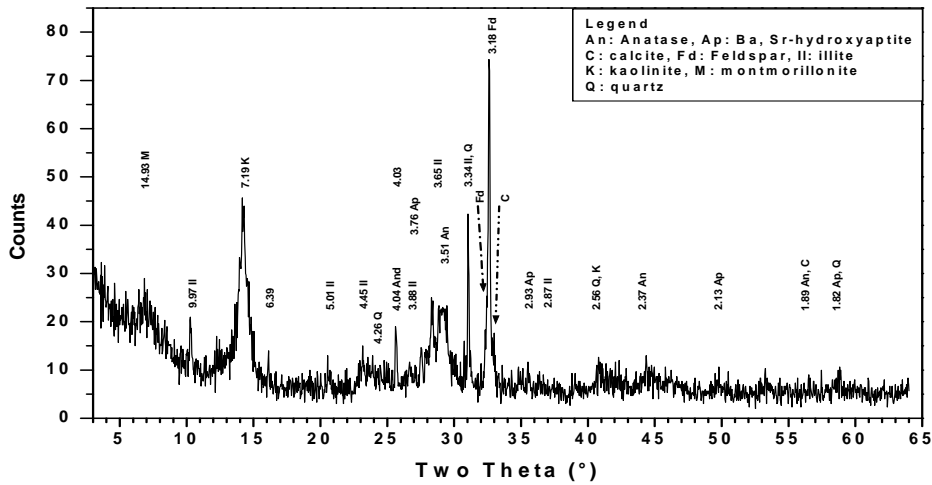


Fig. 1 XRD patterns of crude clay from Bikougou deposit

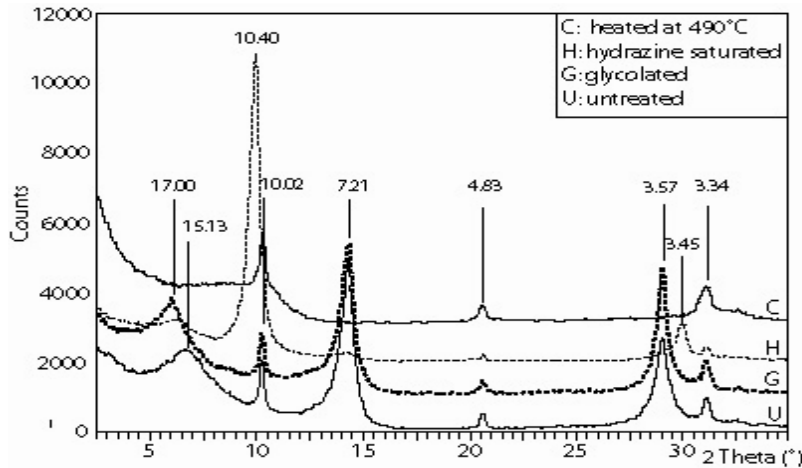


Fig. 2 XRD patterns of clay fraction from Bikougou deposit

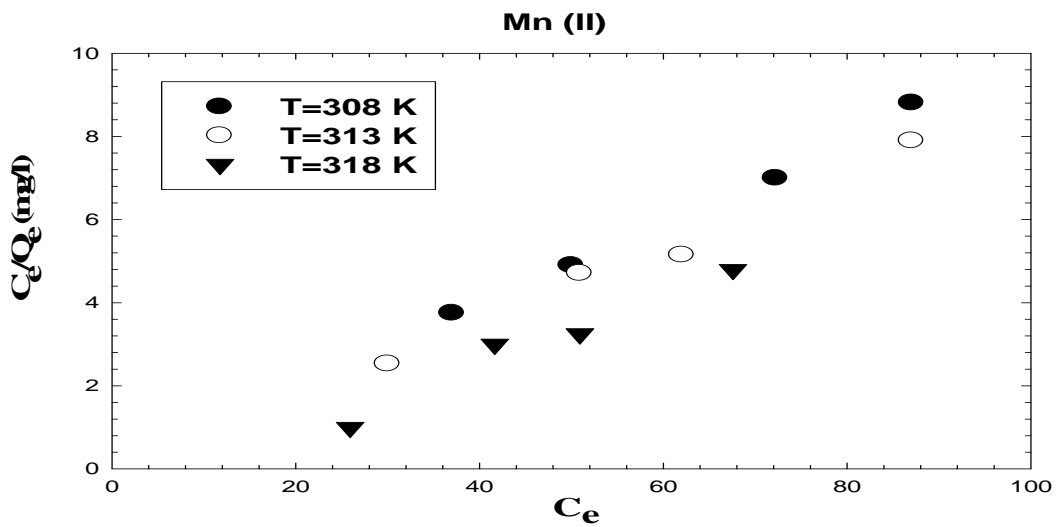
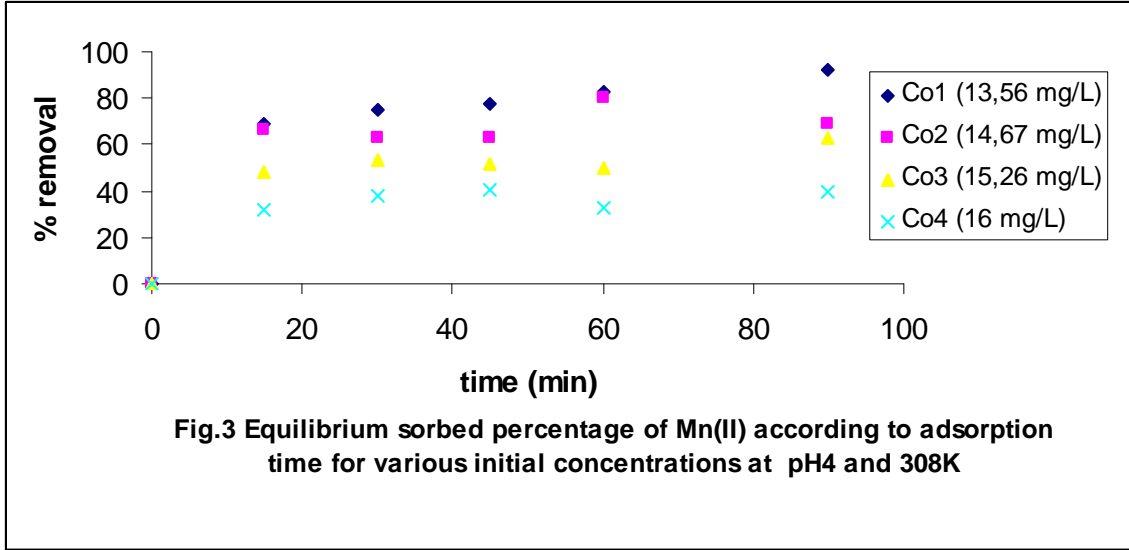


Fig.4 Langmuir plots for Mn (II) ions adsorbed on clay at 308K (initial concentration 66.66, 83.33, 98.148 and 116.66 mg/L) at pH4

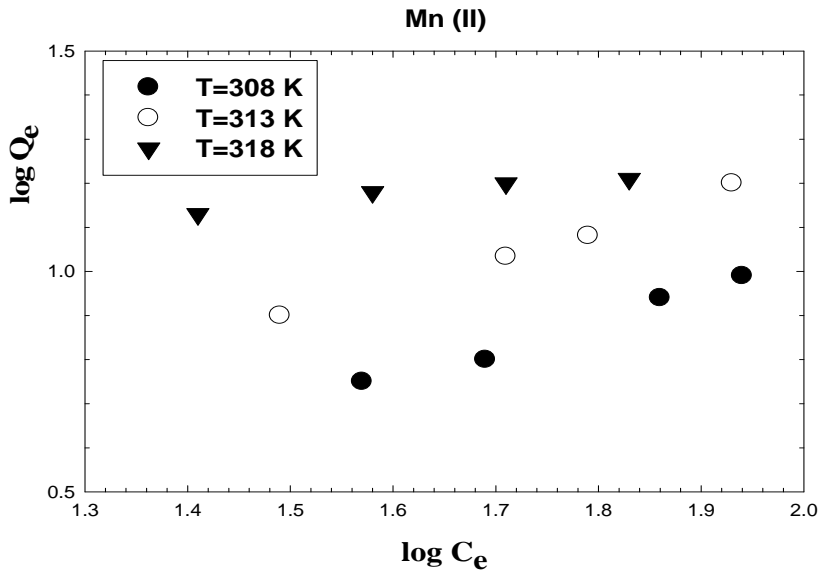


Fig.5 Freundlich plots for Mn (II) ions adsorbed on clay at 308K and at pH4 (initial concentration of Mn(II) ions 66.66, 83.33, 98.148 and 116.66 mg/L)

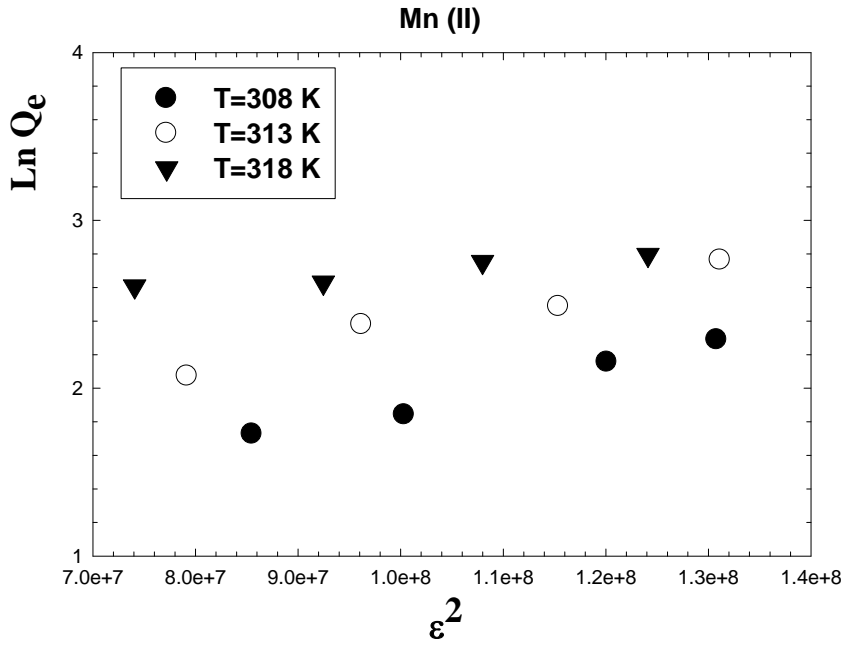


Fig.6 DKR plots for Mn (II) ions adsorbed on clay at 308K and at pH4 (initial concentration of Mn (II) ions 66.66, 83.33, 98.148 and 116.66 mg/L)

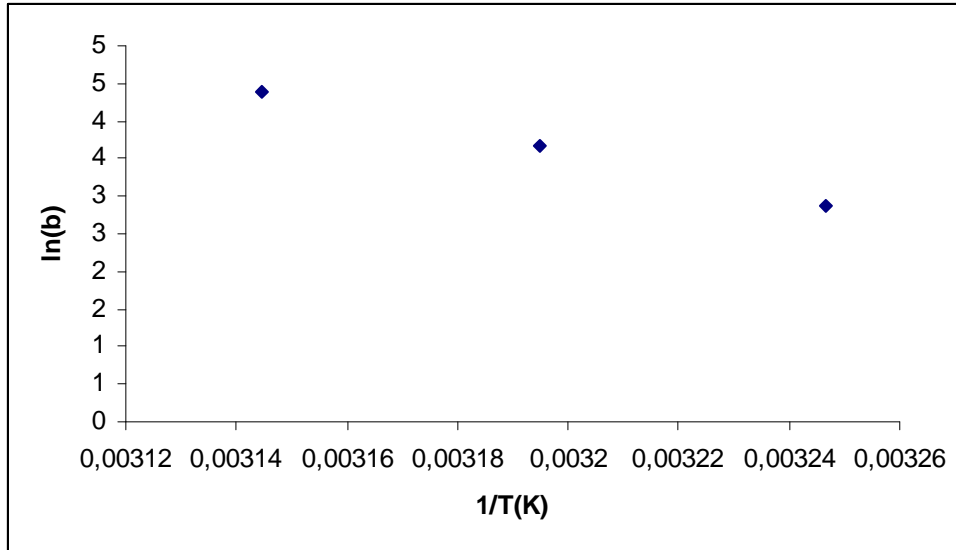
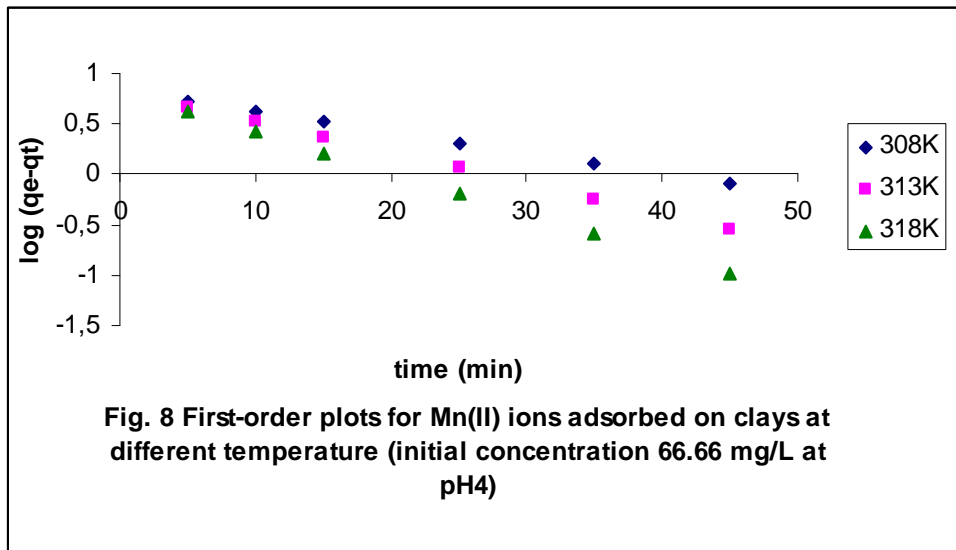


Fig.7 Relationship between Langmuir sorption equilibrium constant and temperature for Mn (II) ions adsorbed on clay at pH4



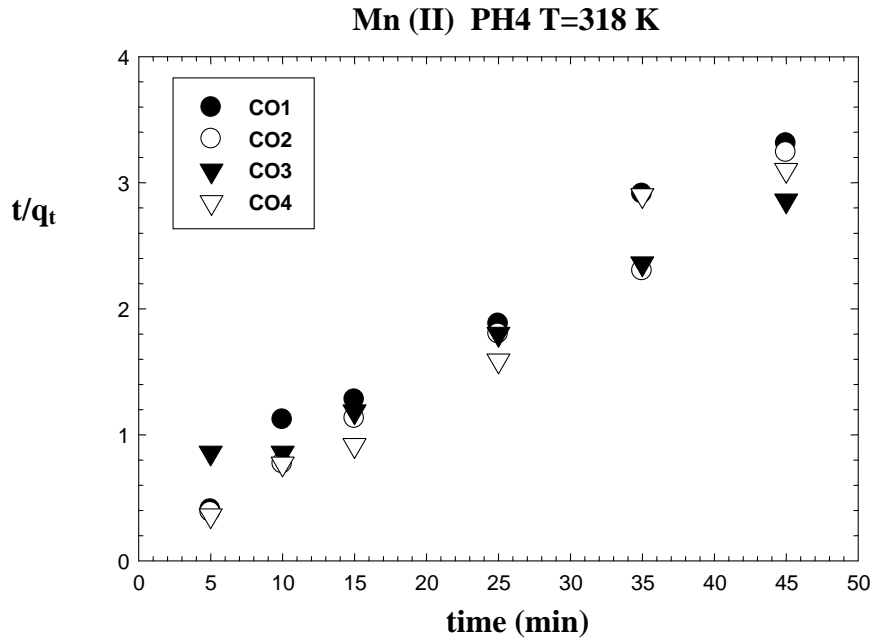


Fig.9 Second-order plots for Mn (II) ions adsorbed on clay at 318K and at pH4 (initial concentration: CO1=66.66 mg/L; CO2=83.33 mg/L; CO3=98.148 mg/L; CO4=116.66 mg/L)

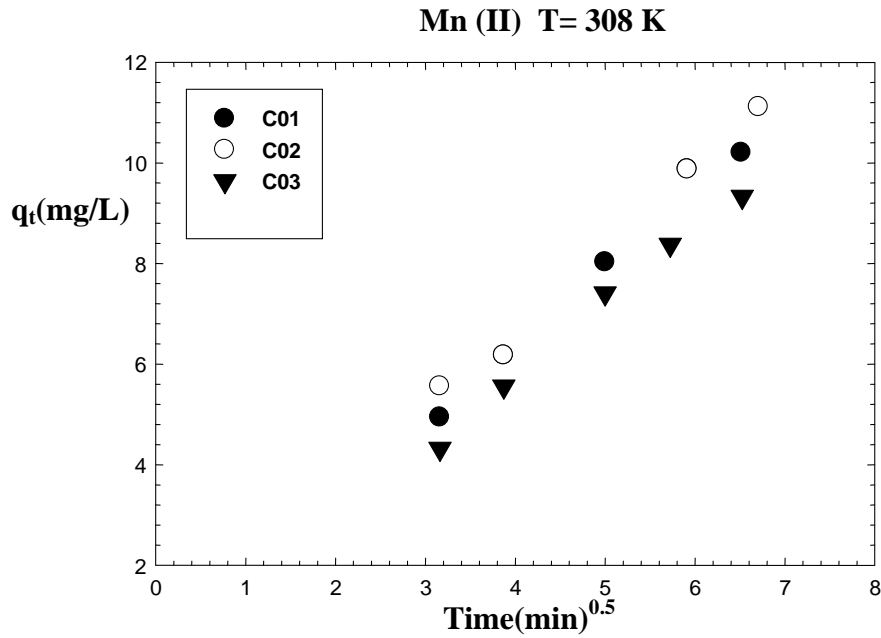


Fig. 10 Intra-particle diffusion plots for Mn (II) ions adsorbed on clays at 308K and at pH4 (initial concentration: CO1=66.66 mg/L; CO2=83.33 mg/L; CO3=98.148 mg/L)

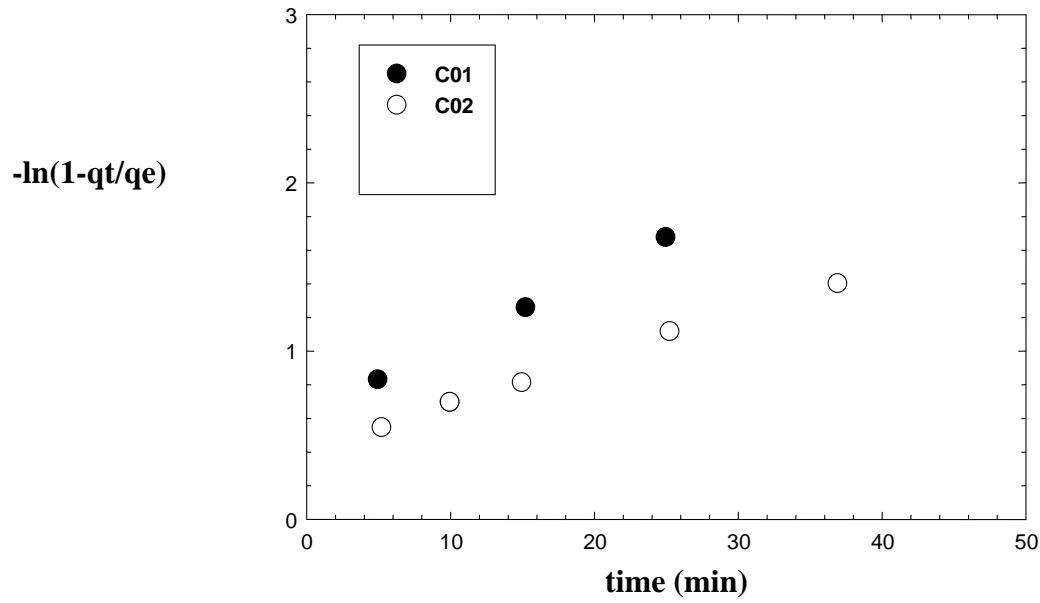


Fig. 11 Liquid film diffusion plots for Mn (II) ions adsorbed on clay at 308K and at pH4 (initial concentration: C01=66.66 mg/L; C02=83.33 mg/L)